ISSN 0016-7029, Geochemistry International, 2022, Vol. 60, No. 4, pp. 363–378. © Pleiades Publishing, Ltd., 2022.
Russian Text © The Author(s), 2022, published in Geokhimiya, 2022, Vol. 67, No. 4, pp. 359–375.

Physicochemical Study of Titanium-Bearing Garnets

L. P. Ogorodova[a, *], Yu. D. Gritsenko[a, b], M. F. Vigasina[a], V. S. Rusakov[c], L. V. Melchakova[a], A. Yu. Bychkov[a], and D. A. Ksenofontov[a]

[a] *Faculty of Geology, Moscow State University, Moscow, 119991 Russia*
[b] *Fersman Mineralogical Museum, Russian Academy of Sciences, Moscow, 119692 Russia*
[c] *Faculty of Physics, Moscow State University, Moscow, 119991 Russia*
**e-mail: logor48@mail.ru*

Received April 5, 2021; revised July 4, 2021; accepted July 8, 2021

Abstract—Four samples of natural Ti-bearing garnets from Odihincha, Maimecha-Kotui alkaline province, Krasnoyarsk Krai, Russia, were studied using electron microprobe analysis, X-ray powder diffraction (XRD), Fourier-transform infrared spectroscopy (FTIR), Raman and Mössbauer spectroscopy, and thermal analysis. The enthalpies of formation from elements were determined with a high-temperature heat-flux Tian–Calvet microcalorimeter by means of the melt solution calorimetry. The first ever values of $\Delta_f H^0_{el}$ (298.15 K) were determined as follows: −5861.1 ± 11.3 kJ/mol for $(Ca_{3.00}Na_{0.02}Fe^{2+}_{0.01})(Fe^{3+}_{1.42}Ti^{4+}_{0.26}Al_{0.21}Mg_{0.04}Fe^{2+}_{0.03}Mn^{2+}_{0.01})[(Si_{2.85}Fe^{3+}_{0.13})O_{11.92}(OH)_{0.08}]$; −5915.2 ± 9.0 kJ/mol for $Ca_{3.01}(Fe^{3+}_{1.27}Ti^{4+}_{0.57}Mg_{0.05}Fe^{2+}_{0.03}Mn^{2+}_{0.01})[(Si_{2.69}Al_{0.16}Fe^{3+}_{0.13}Ti^{4+}_{0.01})O_{11.96}(OH)_{0.04}]$; −5902.5 ± 9.1 kJ/mol for $(Ca_{2.97}Mn^{2+}_{0.02}Fe^{2+}_{0.01})(Fe^{3+}_{1.20}Ti^{4+}_{0.64}Mg_{0.05}Fe^{2+}_{0.04})[(Si_{2.64}Fe^{3+}_{0.23}Al_{0.11}Ti^{4+}_{0.01})O_{11.96}(OH)_{0.04}]$; and −5945.7 ± 10.2 kJ/mol for $(Ca_{2.90}Na_{0.04}Fe^{2+}_{0.03}Mn^{2+}_{0.02}Mg_{0.01})(Fe^{3+}_{0.97}Ti^{4+}_{0.71}Mg_{0.13}Zr_{0.08}Fe^{2+}_{0.05})[(Si_{2.33}Fe^{3+}_{0.32}Ti^{4+}_{0.24}Al_{0.07})O_{11.84}(OH)_{0.16}]$. The standard Gibbs free energies of formation of these garnets were calculated using the values obtained for the formation enthalpies and estimated for the entropies. Also, the enthalpies of formation of the end-members of the isomorphic schorlomite–morimotoite series were derived. The thermodynamic constants were used in quantitative modeling of the stability fields of these minerals.

Keywords: titanium-bearing garnets, schorlomite, morimotoite, XRD, FTIR, Raman and Mössbauer spectroscopy, thermal analysis, thermochemistry, enthalpy of formation, entropy, Gibbs energy of formation

DOI: 10.1134/S0016702922030053

INTRODUCTION

Titanium-bearing garnets are minerals typical of many skarn, metamorphic, and carbonatite deposits and are dominant rock-forming minerals at some of them. However, the composition and properties of these minerals and parameters at which they are formed in nature are disputable, although many microprobe, spectroscopic, and X-ray single-crystal studies have been devoted to these phases. The generalized formula of the minerals of the garnet supergroup is $(X_3)(Y_2)[Z_3]\varphi_{12}$, where *X*, *Y*, and *Z* are dodecahedrally, octahedrally, and tetrahedrally coordinated sites, respectively, and φ is O^{2-}, OH^-, and/or F^- (Grew et al., 2013).

Currently 39 mineral species of the garnet supergroup are known and described, with more than ten of them discovered over the past few years (*IMA List of Minerals*; Krivovichev et al., 2019; Galuskina et al., 2020; Karlsson et al., 2020).

As of 2020, the Commission on New Minerals, Nomenclature, and Classification of the International Mineralogical Associations (CNMNC IMA) had approved three mineral species of titanium-bearing garnets: schorlomite $Ca_3(Ti,Fe^{3+})_2[(Si,Fe^{3+})_3O_{12}]$, morimotoite $Ca_3(Ti,Fe^{2+},Fe^{3+})_2[(Si,Fe^{3+})_3O_{12}]$, and hutcheonite $Ca_3Ti_2[(Si,Al)_3O_{12}]$, whose idealized formulas are, respectively, $Ca_3Ti^{4+}_2[SiFe^{3+}_2O_{12}]$, $Ca_3(Ti^{4+}Fe^{2+})[Si_3O_{12}]$, and $Ca_3Ti^{4+}_2[SiAl_2O_{12}]$. Available data indicate that these minerals are interrelated through continuous solid-solution series with one another and with andradite (Grew et al., 2013; Ma and Krot, 2014).

Schorlomite was first found in Arkansas (Shepard, 1846) and received its name because its resemblance to schorl. Its composition and properties have been refined by J.D. Whitney and K.F Rammelsberg (Whitney, 1849; Rammelsberg, 1850). Morimotoite was discovered at the Fuka calc-skarn occurrence in

Okayama Prefecture, Japan (Henmi et al., 1995). Hutcheonite is an aluminous analogue of schorlomite and was found in 2014 in inclusions of the Allende carbonaceous chondrite, in which this mineral occurs as secondary-alteration phase at contacts between melilite, perovskite, and Ti–Al diopside (Ma and Krot, 2014).

Natural and synthetic Ti-bearing garnets of the andradite–schorlomite–morimotoite series have been extensively studied by X-ray diffraction and by Mössbauer, IR, and Raman spectroscopy (Dowty, 1971; Huggins et al., 1977a, 1977b; Tarte et al., 1979; Schwartz et al., 1980; Henmi et al., 1995; Locock et al., 1995; Peterson et al., 1995; Armbruster et al., 1998; Schingaro et al., 2004; Chakhmouradian and McCammon, 2005; Katerinopoulou et al., 2009; Chukanov, 2014; Antao et al., 2015; Schingaro et al., 2016; Gritsenko, 2018), and their structure and unit-cell parameters were refined in (Peterson et al., 1995; Henmi et al., 1995; Schingaro et al., 2016). The thermodynamic characteristics of minerals of this group were studied only in (Rass and Dubrovinskii, 1997), in which $\Delta_f G^0_{el}$ was calculated at various temperatures by minimizing the Gibbs free energy of hypothetical garnet $Ca_3Ti_2Ti_3O_{12}$, which was referred to as *schorlomite* by the authors. However, this formula is inconsistent with the IMA nomenclature for the garnet supergroup (Grew et al., 2013). The origin of this phase was thermodynamically simulated for the model discussed in (Rass and Dubrovinskii, 1997), in which the Ti^{4+} and Ti^{3+} completely substituted Si^{4+} and Fe^{3+} on the tetrahedrally and octahedrally coordinated sites in the garnet structure. The authors have demonstrated that this phase can be formed only at higher temperatures and under more reduced conditions than those of perovskite, which is known to crystallize under highest temperatures and most reducing conditions (in such rocks as, for example, kimberlite and picrite). However, no such extreme parameters can occur in any known geological processes and environments on the Earth, and this explains why $Ca_3Ti_2^{3+}Ti_3^{4+}O_{12}$ cannot be found as naturally occurring mineral. Moreover, Ti^{3+} still has not been identified in any naturally occurring terrestrial garnets (Locock, 2008; Grew et al., 2013).

The aim of our study was a comprehensive experimental study of physicochemical properties of natural samples of Ti-bearing garnets, including determining their standard enthalpies of formations and calculating the Gibbs free energies from the obtained values of the enthalpy of formation and the entropies of the minerals.

EXPERIMENTAL

Four fragments of large (5–18 cm) unzoned garnet crystals were hand-picked from the material of a pegmatoid vein in the contact zone between melilite rocks and jolite of the Odikhincha alkaline–carbonatite massif in the Maymecha–Kotui alkaline province in Krasnoyarsk Krai, Russia. Samples I and III were taken from a large pegmatite vein: sample I was taken from its central part (which consisted of garnet, fine-grained "sugary" apatite, and phlogopite), and sample III was from a peripheral zone (in which this mineral occurs together with large crystals of apatite, phlogopite, long-prismatic apatite, and magnetite). Samples II and IV were collected in the central portion of a nepheline–diopside–calcite pegmatoid vein, in which garnet occurs as large (up to 10 cm) crystals in calcite and fills the intergranular space between euhedral nepheline crystals (in sample IV) or forms garnet–apatite aggregates in intergrowths with diopside and nepheline (sample III). Samples were made available for this research by courtesy of the Research Foundation of the Fersman Mineralogical Museum, Russian Academy of Sciences (sample I, No. FN 281; sample II, No. FN 280, sample III No. FN 279, and sample IV No. FN 278). Homogeneous fragments of the crystals devoid of visible solid and/or liquid inclusions (larger than 3 μm) were hand-picked for their further study under an AXIOPLAN 2 IMAGING (Germany) optical microscope.

The *X-ray powder diffraction (XRD) study* was carried out in a STOE-STADI MP (Germany) diffractometer equipped with a curved Ge (111) monochromator, which emits strictly monochromatic $CoK\alpha_1$ radiation (λ = 0.178897 Å). The data were acquired within the 2θ range of 15° to 70° by successively covering scanning ranges using a linear positively sensitive detector whose capture angle 2Θ was 5° and the channel width was 0.02°. The counting time was 10 s at each individual spot. The unit-call parameters of the garnet were calculated using the WinXPow (WinXPow Software STOE and CIE GmbH 2002) and XPowINDEX (which includes Werner's TREOR, Visser's ITO and Louer's DICVOL) program packages.

The *chemical analysis* was conducted on a CAMEBAX SX-50 (France) microprobe at an accelerating voltage of 15 kV and a beam current of 30 nA. The standards were natural minerals: pyrope $Mg_3Al_2Si_3O_{12}$ for Mg and Si, almandine $Fe_3Al_2Si_3O_{12}$ for Al and Fe, grossular $Ca_3Al_2Si_3O_{12}$ for Ca, uvarovite $Ca_3Cr_2Si_3O_{12}$ for Cr, spessartine $Mn_3Al_2Si_3O_{12}$ for Mn, zircon $ZrSiO_4$ for Zr, and cassiterite SnO_2 for Sn; as well as synthetic $KTiPO_5$ for Ti and VO_3 for V.

The *thermal behavior* of the garnets was studied on a Q-1500 D (Hungary) derivatograph at temperatures changed from room temperature to 1273 K, at a heating rate of 20 K/min. The mass of the sample was 280–340 mg. The equipment was calibrated using standard references sample provided by the manufacturing company, by the phase transitions α-quartz → β-quartz and by the weight loss of a calcium oxalate standard reference sample. The measurements were accurate to $\pm 4 \times 10^{-2}$ mg, i.e., ~0.01% for a 300-mg sample.

The *IR spectroscopic study (FTIR)* was done on a FSM-1201 (Russia) Fourier-transform IR spectrometer in transmission mode, at room temperature, in air, within the wavenumber range of 400 to 4000 cm^{-1}, accurate to ± 1 cm^{-1}. Samples for this study were prepared in the form of suspensions of the powdered minerals (3–5 mg) in paraffinic oil and were applied to a KBr platelet, which were then mounted on the specialized holder perpendicular to the IR radiation beam. The working diameter of the beam was 5 mm.

The *Raman spectroscopic study* was conducted on a EnSpectr R532 (Russia) Raman spectrometer. The wavelength was 532 nm, and the output laser power was 15–30 MW. The holographic diffraction grating had 1800 grooves per mm (g/mm), the spectral resolution was 6 cm^{-1}, and the focal spot was approximately 10 μm at a 40× magnification. The spectra were recorded within the range of 100 to 4000 cm^{-1} from randomly oriented crystals, the exposure time was 1–1.5 s, the signal was averaged over 80–100 exposures. The equipment was calibrated on the silicon scattering line with a frequency of 520.5 cm^{-1}.

The *gamma-resonance spectroscopic study* of the garnets was conducted on a MS1104Em (Russia) Mössbauer spectrometer in a constant acceleration mode, with a triangular configuration of the Doppler velocity change of the source relative to the absorber. The measurements were carried out in a transmission geometry, at room temperature, with a standard radioactive source of ^{57}Co in Rh matrix, at an activity of ~7 mCi. The Mössbauer spectrometer was calibrated at room temperature, using a standard α-Fe absorber. Powdered samples of the garnets were pressed into pellets of specified thickness to reach optimal measurement conditions.

The raw spectra were processed with the least-squares method with an approximation of a Foigt pseudoresonance profile $PV(x, \alpha, \Gamma)$, using the SpectrRelax software (Matsnev and Rusakov, 2012)

$$PV(x,\alpha,\Gamma) = (1-\alpha)L(x,\Gamma) + \alpha G(x,\Gamma), \qquad (1)$$

where $L(x,\Gamma)$ and $G(x,\Gamma)$ are the normalized Lorentzian and Gaussian functions, respectively, α is the conversion coefficient, and Γ is the full width half maximum (half-width) of the line.

The *thermochemistry* study of the garnets was carried out using a Setaram (France) Tian–Calvet heat-conducting microcalorimeter. The solvent was melt of the composition $2PbO \cdot B_2O_3$, which had been prepared by fusing stoichiometric amounts of Pb oxide and boron hydroxide at 1073 K. The experiments were conducted in air, by dropping the samples [in the form of fragments of optically isotropic crystals 1.2–6.3 ($\pm 2 \times 10^{-3}$) mg from room temperature to the calorimeter with melt at $T = 973$ K. The measured heat effect involved the enthalpy of the sample and its dissolution enthalpy $\Delta H = [H^0(973\text{ K}) - H^0(298.15\text{ K})) + \Delta_{dissol}H^0(973\text{ K})]$. When 30–35 g of the solvent melt were used and six to eight experiments were made, the ratio of the dissolved compound to solvent can be regarded as that of infinitely diluted solution, whole mixing enthalpy is negligibly small. The tool was calibrated on Pt, and data on its enthalpy at $T = 973$ K were compiled from (Robie and Hemingway, 1995). Using the acquired experimental data and based on the thermochemical cycle, which involved the dissolution of the mineral and its components, we calculated the enthalpy of formation of four titanium-bearing garnets.

The Mössbauer spectrometer is installed at the Faculty of Physics of the Lomonosov Moscow State University, and the rest of the equipment utilized in this research is situated at the Faculty of Geology of the Lomonosov Moscow State University.

RESULTS AND DISCUSSION

Samples

X-ray diffraction study. The X-ray diffraction patterns of the garnets are shown in Fig. 1. In terms of X-ray diffraction characteristics, sample I is close to andradite, in compliance with data in *RRUFF (Database of Raman Spectroscopy, X-ray Diffraction and Chemistry of Minerals;* card R050377*)* and MINCRYST *(Crystallographic and Crystal-Chemical Database for Minerals and Their Structural Analogues;* card 208). Sample IV is similar to schorlomite (MINCRYST card 9909). The X-ray powder diffraction patterns of samples II and III are similar to one another, and the minerals can be classed with intermediate members of the andradite–schorlomite–morimotoite series.

The calculated unit-cell parameter *a* and the unit-cell volume *V* are reported, along with the volumes of the Ti-bearing garnets, in Table 1. The values of *a* of samples I and IV are analogous to the parameters of andradite and schorlomite, respectively. As expected, the unit-cell parameters of the garnets increase with increasing concentration of the Ti component. Sample IV, which is the closest to schorlomite, has the greatest *a* parameter.

Chemical analysis. Table 2 reports average (of individual analyses at three analytical spots) compositions of samples I, II, III, and IV (the latter is an average of nine spot analyses). According to these data, sample I is the closest to andradite, sample IV most closely approaches schorlomite, and samples II and III are similar in chemical composition and can be identified with intermediate members of the andradite–schorlomite–morimotoite series of solid solutions.

Thermal analysis. The thermogravimetric curves of the garnets (Fig. 2) indicate minor mass losses (about 0.1–0.3 wt %) at temperatures of 473–873 K. These data are consistent with those of thermal studies of synthetic garnets of the series grossular $Ca_3Al_2[SiO_4]_3$–katoite $Ca_3Al_2[(SiO_4)_y(OH)_{4(3-y)}]$ (Rivas-Mercury et al., 2008) and andradite $Ca_3Fe_2^{3+}[SiO_4]_3$–Fe-

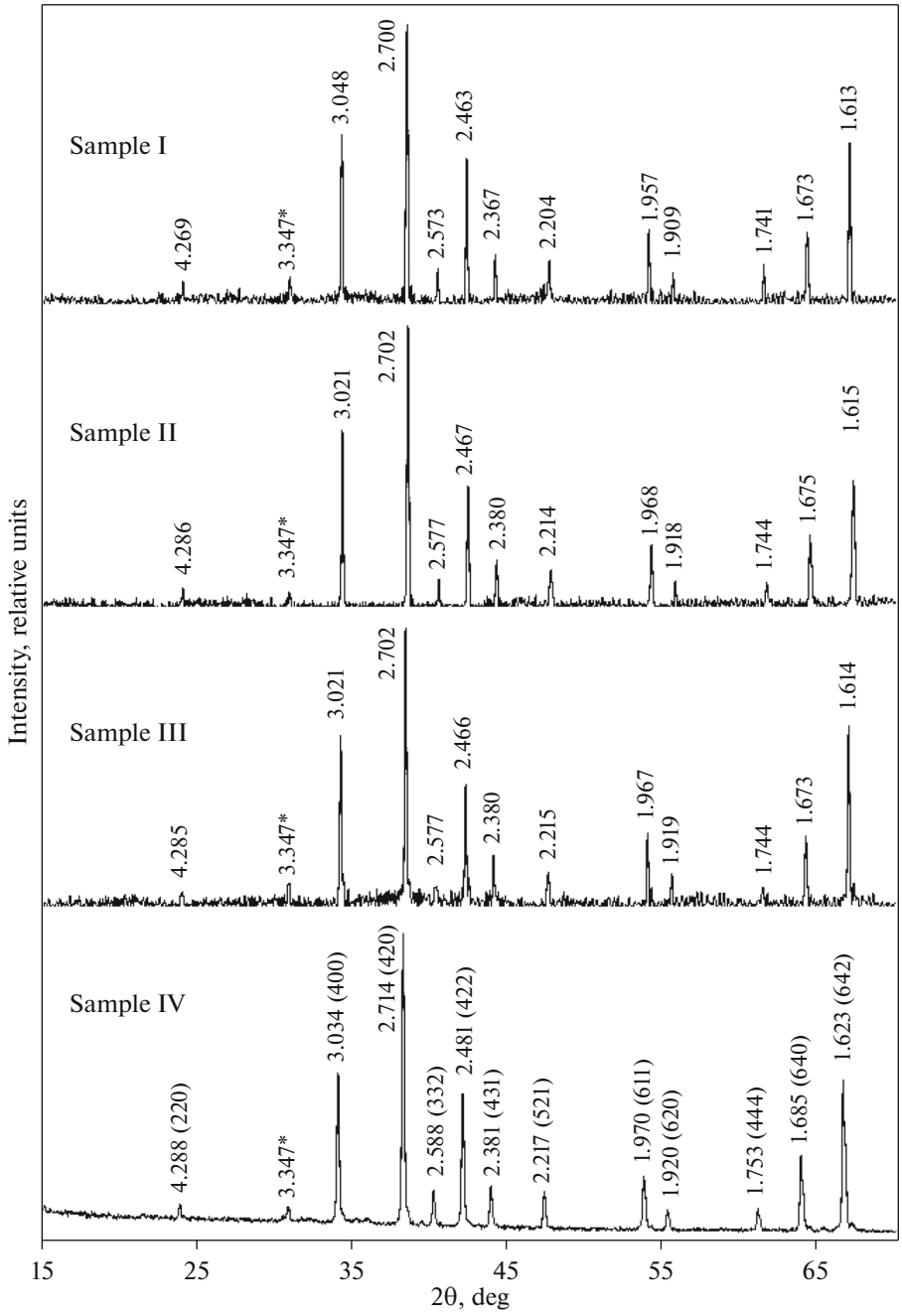

Fig. 1. X-ray powder diffraction patterns of the Ti-bearing garnets. Spacings are specified in Å. * Quartz employed as an internal standard.

katoite $Ca_3(Al_xFe_{1-x})_2[(SiO_4)_y(OH)_{4(3-y)}]$ (Dilnesa et al., 2014) ($0 < y < 3$). Data reported in these publications indicate that the mass losses of our garnet samples can be explained by hydroxyl loss from them, and the samples themselves shall likely be attributed to OH-bearing garnets (Grew et al., 2013). According to the model currently adopted for hydroxyl-bearing garnets, they are formed by the schematic reaction $[SiO_4]^{4-} \leftrightarrow (O_4H_4)^{4-}$ (Schingaro et al., 2016).

IR spectroscopy. The acquired IR absorption spectra of samples I, II, and III (Fig. 3) are similar to one another and to that of no. Sio9 (Chukanov, 2014) of Ti-bearing andradite from the Kovdor alkaline ultramafic complex in the Kola Peninsula, Russia, and the spectra of synthetic Ti-bearing garnets (Tarte et al., 1979).

The spectra can be described with regard to results in (Tarte et al., 1979; Hofmeister and Chopelas, 1991;

Kurazhkovskaya and Borovikova, 2002). The region of valence triply degenerate oscillations of SiO_4 tetrahedrons shows two broad absorption bands with maxima at approximately 808–817 and 886–887 cm^{-1}. The absence of splitting of the low-frequency components (as is typical of the end members of the andradite–schorlomite–morimotoite series) and the occurrence of poorly discernible shoulders of the high-frequency components (911–914 and 940–941 cm^{-1}) provide evidence of the presence of the Fe^{3+} and Al cations at the tetrahedrally coordinated site. The presence of cations with charges other that 4+ at the tetrahedrally coordinated site, with an unbalanced charge, results in strain and some deformation of the crystal structure. Changes in the bond lengths and angles relative to their equilibrium values induce changes in the oscillation frequencies of these structural elements, and this is reflected in the slight shifts of the corresponding absorption bands. As a result, the absorption bands widen, begin to overlap one another, and consequently, the whole spectrum contour is smoothed.

The triply degenerate deformation oscillations of the tetrahedrons are also registered in the spectral region below 600 cm^{-1} as two low-intensity bands with maxima at about 589–591 and 477–478 cm^{-1} and two medium-intensity lines with maxima at about 511–512 and 431–434 cm^{-1}. The two broad low-intensity absorption bands with maxima at 651–656 and 691–695 cm^{-1} are referred to the valence oscillations of $(Fe^{3+},Al)O_4$ tetrahedrons.

The spectrum of sample IV (Ti richest garnet with the maximum Fe^{3+} and Ti^{4+} concentrations) is closely similar to the spectrum of garnet TiSi169 (Chukanov, 2014), which was named schorlomite, from the Afrikanda alkaline massif, Kola Peninsula, Russia. However, the composition of sample TiSi169 was recalculated to 25% of the schorlomite end member, 40% morimotoite, and 35% andradite + grossular and corresponds, according to the current nomenclature (Grew et al., 2013) it must be related to the morimotoite mineral species. The spectrum of sample IV is somewhat different from that of samples I, II, and III. The high-frequency component of the triply degenerate oscillations of the tetrahedrons in the range of 890–960 cm^{-1} has lost its clearly seen maximum and is more diffuse, which indicates that silicon cations at the tetrahedral site are largely substituted for other cations. At frequencies lower than 500 cm^{-1}, the intensity of the band at 475 cm^{-1} decreases, and the other band slightly shifts toward lower frequencies, to 426 cm^{-1}. The intensity of the absorption band referred to the valence oscillations of $(Fe^{3+},Al)O_4$ tetrahedrons, with a frequency of about 649 cm^{-1}, slightly increases. Absorption bands of very low intensity corresponding to valence oscillations of the OH group (at 3410, 3507, and 3563 cm^{-1}) were registered in the high-frequency part of the spectrum only

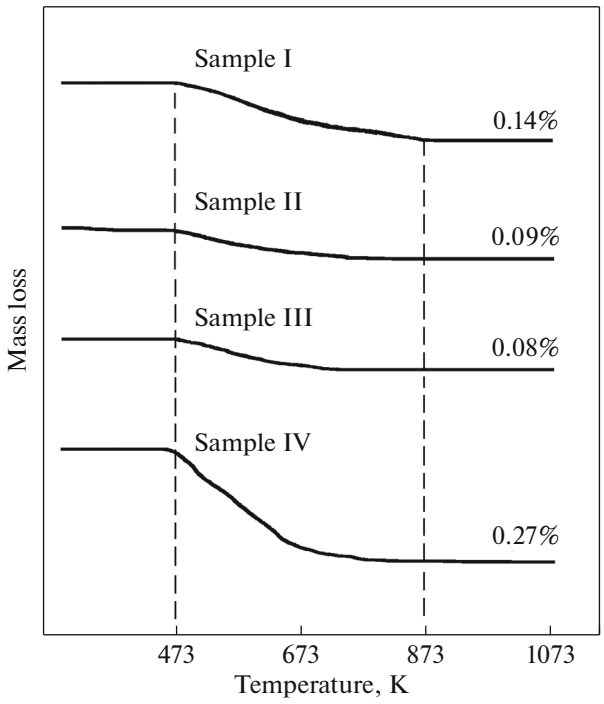

Fig. 2. DTA curves of the Ti-bearing garnets.

Table 1. Unit-cell parameters [a] and molar volume [b] of the studied garnets

Sample	*a*, Å	*V*, Å^3	V_m^0(298.15 K), cm^3/mol
I	12.043(7)	1747(3)	131.5(2)
II	12.077(7)	1762(3)	132.6(2)
III	12.097(7)	1770(3)	133.3(2)
IV	12.144(7)	1791(3)	134.8(2)

[a]Cubic system, space group *Ia*3*d*. [b]Calculated by the formula V_m^0 (298.15 K) = a^3N/Z, where $Z = 8$, and N is the Avogadro constant.

Table 2. Chemical composition (wt %) of the garnets from the Odikhincha massif: microprobe analyses and thermal-analysis data

Oxide	Sample I	Sample II	Sample III	Sample IV
Na_2O	0.21	n.d.	n.d.	n.d.
MgO	0.32	0.49	0.42	1.12
CaO	33.53	33.24	32.65	32.11
MnO	0.16	0.17	0.23	0.34
Fe_2O_3	25.31	22.58	23.29	21.67
Al_2O_3	2.13	1.52	0.99	0.71
ZrO_2	0.09	0.07	0.09	1.85
TiO_2	4.05	9.23	10.30	15.01
SiO_2	34.09	31.64	30.98	27.56
H_2O	0.14	0.09	0.08	0.27
Total	100.03	99.03	99.03	100.88

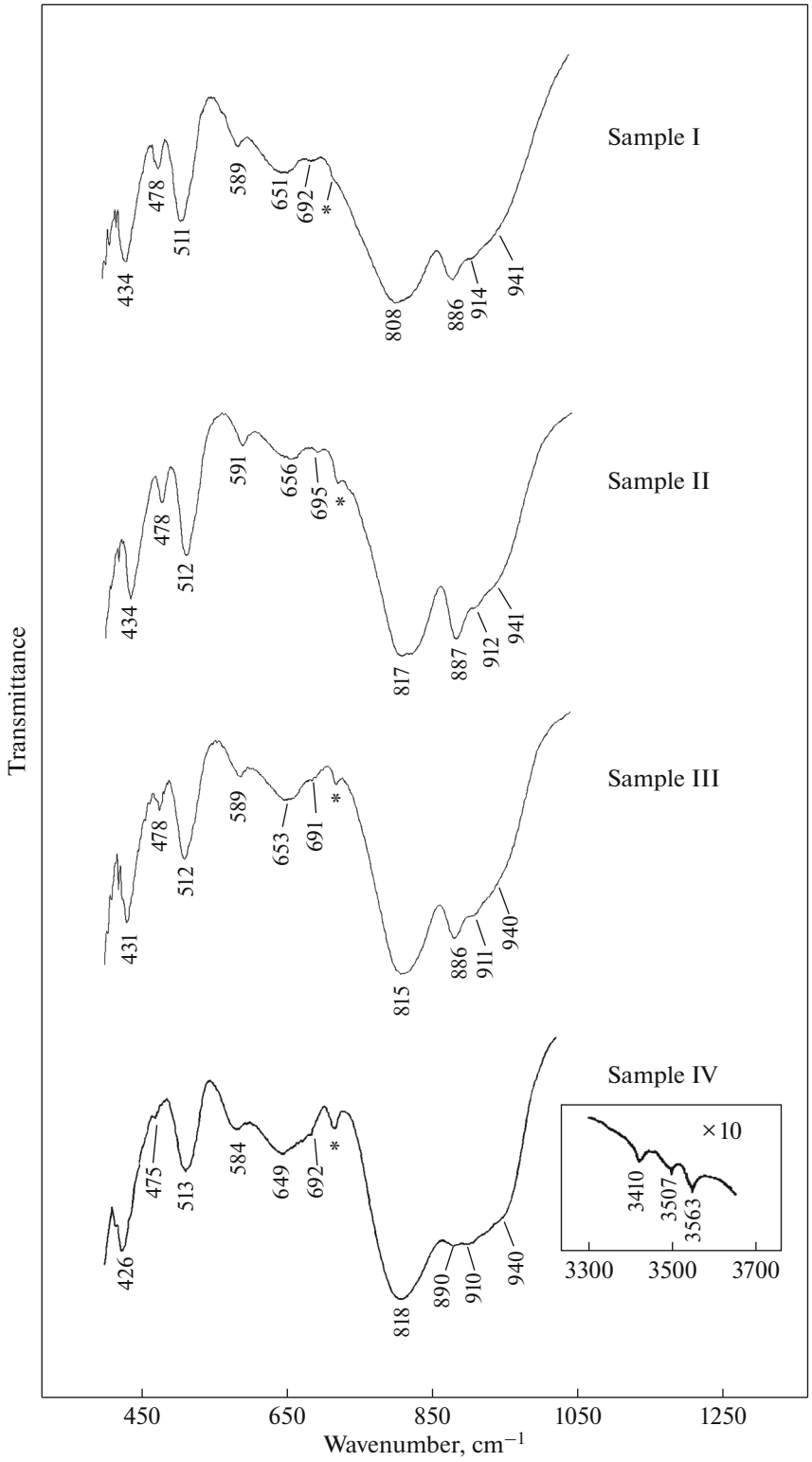

Fig. 3. IR spectra of the Ti-bearing garnets.

for sample IV, which contains the highest concentrations of OH groups (Fig. 3, inset).

The occurrence of absorption bands in the regions of valence oscillations of OH groups indicates that the structure of sample IV contains defects typical of hydrogarnets, in which four OH^- ions substitute the $[SiO_4]^{4-}$ anion at the tetrahedrally coordinated site. Some publications (Bell and Rossman, 1992; Arm-

bruster and Geiger, 1993; Beran and Libowitzky, 2006) present results of studies of hydrogarnets of the grossular–andradite series in which IR absorption bands at 3512–3525 cm^{-1} are thought to be related to the occurrence of the Ti^{4+} cation at the octahedral site. When andradite (Armbruster and Geiger, 1993) and schorlomite (Locock et al., 1995) were studied, an absorption band with a maximum at about 3564–3565 cm^{-1} was registered, which was related by these authors to the occurrence of octahedrally coordinated Ti^{4+}. Based on the data presented above, the three absorption bands in the high-frequency region of the spectrum of sample IV (at about 3410, 3507, and 3565 cm^{-1}) may also be related to the presence of defects of the type $(OH)_4^{4-}$ in the structure. The occurrence of the three absorption bands in the spectrum of this sample can be reasonably explained by the different cation occupancy (Ti^{4+}, Fe^{3+}, and Mg) of the nearest octahedral sites (Reynes et al., 2018).

Raman spectroscopy. The Raman spectra of the samples are displayed in Fig. 4. The spectrum of sample I is closely similar to the spectrum of Ti-bearing andradite of analogous chemical composition from the Zlatoust area in the Southern Urals, Russia (*RRUFF, Database of Raman Spectroscopy, X-ray Diffraction and Chemistry of Minerals*; card No. R050377). The spectrum of sample IV is close to that of schorlomite from Magnetite Cove in Arkansas, United States (*RRUFF*, card No. R060125). No Raman lines related to the oscillations of hydroxyl groups were recorded in the spectra of any of the samples, which is explained by that the concentrations of the hydroxyl group in the samples are below the sensitivity of the Raman spectral method (<0.3 wt % according to the thermogravimetric data). The spectral region of structural oscillations (<1000 cm^{-1}) can be provisionally subdivided into four segments (Moore, 1971; Kolesov and Geiger, 1998; Katerinopoulou et al., 2009). One of them, which is the widest and most abundant part of the spectrum, includes Raman lines within the range of 965 to 800 cm^{-1}, which correspond to internal asymmetric and symmetric valence oscillations of SiO_4 tetrahedrons (Hofmeister and Chopelas, 1991). The valence oscillations of $Fe^{3+}O_4$ tetrahedrons (Katerinopoulou et al., 2009) lie within the range of 740 (sample I) to 759 cm^{-1} (sample IV), and an increase in Fe concentration at the tetrahedral site (from 0.13 p.f.u. in sample I to 0.32 p.f.u. in sample IV) leads to an increase in the frequency of the valence oscillations of the $Fe^{3+}O_4$ tetrahedrons. The second spectral region (from 440 to 650 cm^{-1}) includes lines corresponding to the inner symmetrical and asymmetrical deformation oscillations of SiO_4 tetrahedrons (Katerinopoulou et al., 2009). The third, narrow, range of 300 to 370 cm^{-1} corresponds to the lines of librational oscillations of tetrahedral structural units. The scattering lines of translational oscillations of the tetrahe-

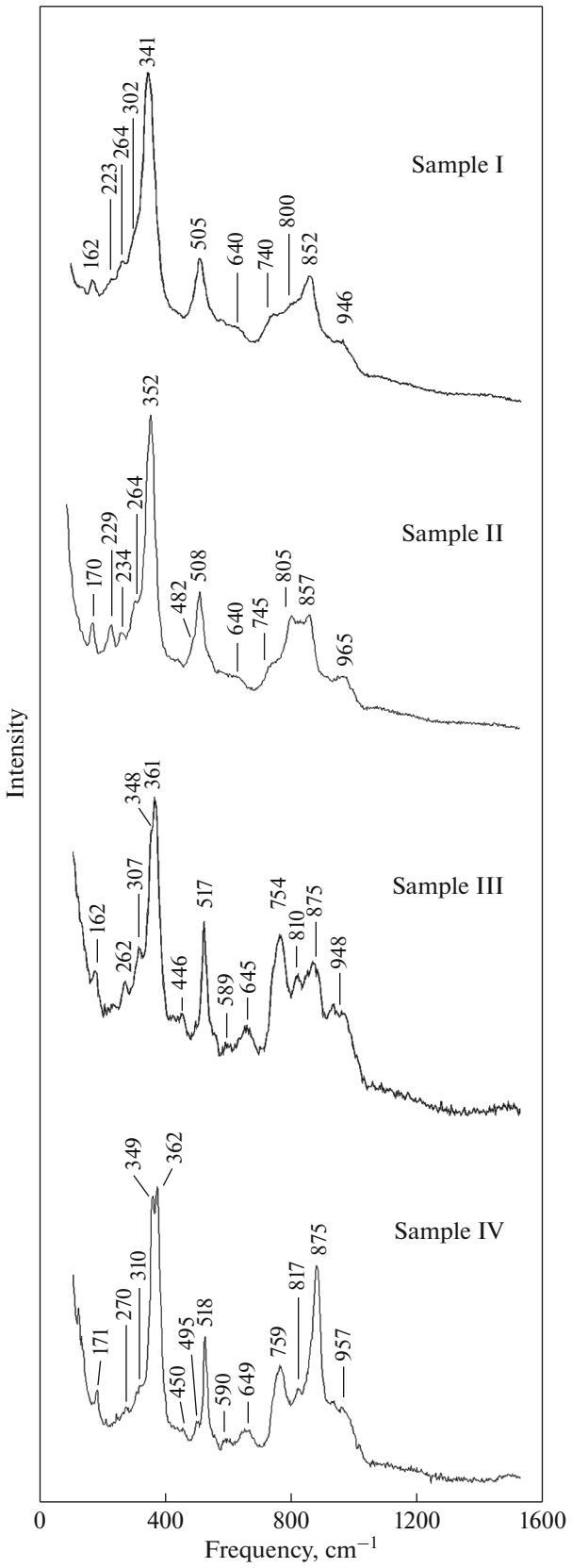

Fig. 4. Raman spectra of the Ti-bearing garnets.

Table 3. Parameters of the Mössbauer spectra of ^{57}Fe in the studied garnets

No.	Quadrupole doublets	Parameters	Sample I	Sample II	Sample III	Sample IV
1	$Fe^{3+}(Y)$	*IS*, mm/s	0.41(1)[a]	0.41(1)	0.41(1)	0.42(1)
		QS, mm/s	0.57(1)	0.58(2)	0.58(1)	0.61(1)
		A, %	76.4(1.1)	77.6(7)	67.0(6)	54.4(1.3)
2	$Fe^{3+}(Y)$	*IS*, mm/s	0.38(1)	0.38(2)	0.38(2)	0.35(1)
		QS, mm/s	0.82(1)	0.84(1)	0.82(1)	0.73(1)
		A, %	11.5(1.0)	10.1(6)	15.8(5)	15.2(1.4)
3	$Fe^{3+}(Z)$	*IS*, mm/s	0.21(1)	0.22(2)	0.21(2)	0.22(2)
		QS, mm/s	1.35(1)	1.35(1)	1.33(1)	1.27(1)
		A, %	8.0(4)	8.2(5)	11.6(2)	19.9(6)
4	$Fe^{3+}(Z) \leftrightarrow Fe^{2+}(X)$	*IS*, mm/s	0.69(3)	0.79(10)	0.64(1)	0.77(2)
		QS, mm/s	2.07(5)	2.28(10)	1.96(2)	2.13(3)
		A, %	1.1(1)	0.7(1)	1.8(2)	3.6(1)
5	$Fe^{3+}(Z) \leftrightarrow Fe^{2+}(Y)$	*IS*, mm/s	0.55(2)	0.61(2)	0.52(1)	0.67(1)
		QS, mm/s	1.56(4)	1.63(4)	1.60(2)	1.55(2)
		A, %	2.0(2)	2.3(1)	2.4(2)	5.5(1)
6	$Fe^{2+}(Y)$	*IS*, mm/s	1.16(2)	1.17(2)	1.20(1)	1.12(3)
		QS, mm/s	3.55(4)	3.55(3)	3.51(2)	3.12(5)
		A, %	1.0(1)	1.1(1)	1.4(1)	1.5(1)
7	Full width half maximum	Γ, mm/s	0.28(2)	0.28(1)	0.28(1)	0.32(1)
8	Resonance line shape parameter	α	0.00(2)	0.03(1)	0.02(1)	0.05(2)
9	Pearson criterion	χ^2	1.01	1.12	1.23	1.48

drons and cations in *X* sites lie in the region below 300 cm^{-1}. Cations occupying octahedral sites in the garnet structure are not involved in the oscillations active at Raman light scattering.

Mössbauer spectroscopy. The results of the measurements and their mathematical processing done to determine the valence states of the iron ions and their surroundings are displayed in Fig. 5. The experimental spectra were approximated by a superposition of six quadrupole symmetrical doublets. The parameters of these doublets (isomer shift *IS*, quadrupole splitting *QS*, full width half maximum (half-width) Γ, relative area *A*, and the α parameter of the resonance line) are presented in Table 3. The approximation of the experimental spectrum by six doublets results in an acceptable value of the Pearson criterion χ^2 ($\chi^2 = 1.01–1.48$) and the absence of any significant systematic deviations of the experimental spectrum from its enveloping curve drawn based on the mathematical processing data (Fig. 5).

Four of the six quadrupole doublets obtained by analyzed the Mössbauer spectrum can be unambiguously (based of comparison with data on superfine parameters according to Menil, 1985) attributed as follows: doublet nos. 1 and 2 (Table 3, Fig. 5) to Fe^{3+} at site *Y* (octahedral coordination), doublet no. 3 to Fe^{3+} at site *Z* (tetrahedral coordination), and doublet no. 6 to Fe^{2+} at site *Y* (octahedral coordination). As seen in Table 3, doublets nos. 4 and 5 are characterized by isomer shifts of 0.69 and 0.55 mm/s, respectively. These values are intermediate between the values of isomer shifts for Fe^{3+} and Fe^{2+} and shall likely be attributed to Fe atoms of valence intermediate between 2+ and 3+ because of the thermally activated delocalization of the electrons. With regard to the crystal structure of garnet, it is reasonable to propose two hypothetical scenarios for electron transfer between crystallographic sites with the involvement of tetrahedrally coordinated Fe^{3+}: (1) $Fe^{3+}(Z) \leftrightarrow Fe^{2+}(X)$ and (2) $Fe^{3+}(Z) \leftrightarrow Fe^{2+}(Y)$. Because the average distance between Fe and O atoms in the dodecahedron is greater than that in the octahedron, the isomer shift for doublet no. 4 is greater than that for doublet 5 (Table 3), and doublets nos. 4 and 5 can thus be assigned to a charge transfer according to the schemes $Fe^{3+}(Z) \leftrightarrow Fe^{2+}(X)$ and $Fe^{3+}(Z) \leftrightarrow Fe^{2+}(Y)$, respectively.

Our study allowed us to determine the concentration of Fe^{2+} and Fe^{3+} at crystallographic sites *X, Y*, and *Z* in the studied garnet samples. The relative areas *A* of

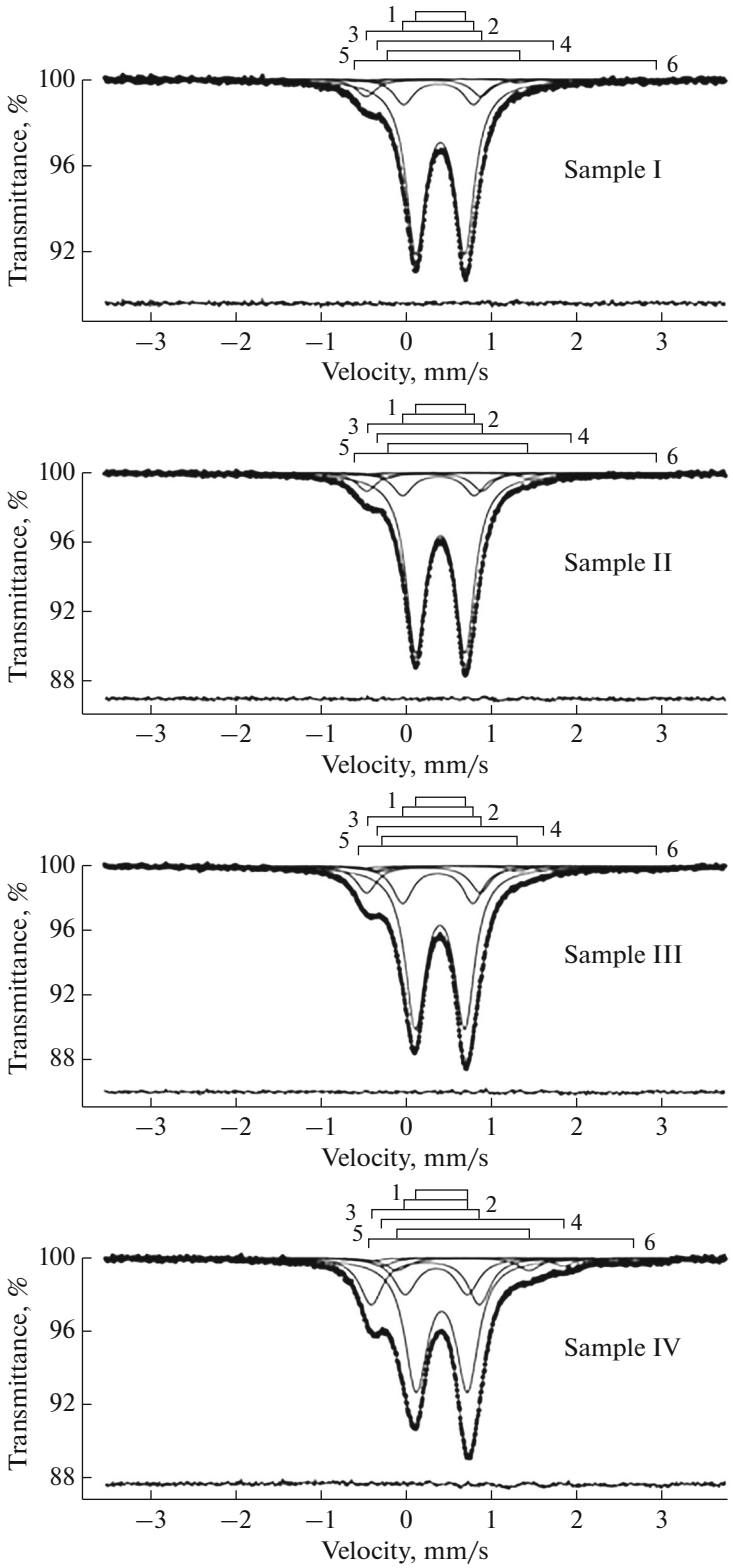

Fig. 5. Mössbauer spectra of the Ti-bearing garnets.

Table 4. $Fe^{(2+/3+)}(X/Y/Z)/\sum Fe$ (%) ratios of the studied garnets calculated from Mössbauer spectroscopic data

No.	Quadrupole doublets	Sample I	Sample II	Sample III	Sample IV
1	$Fe^{3+}(Y)$	76.8(1.1)	78.0(7)	67.5(6)	55.0(1.3)
2	$Fe^{3+}(Y)$	11.6(1.0)	10.2(6)	15.9(5)	15.4(1.4)
3	$Fe^{3+}(Z)$	7.5(4)	7.7(5)	10.9(2)	18.8(6)
4	$Fe^{3+}(Z) \leftrightarrow Fe^{2+}(X)$	1.2(1)	0.8(1)	2.0(2)	3.9(1)
5	$Fe^{3+}(Z) \leftrightarrow Fe^{2+}(Y)$	1.9(2)	2.2(1)	2.3(2)	5.4(1)
6	$Fe^{2+}(Y)$	1.0(1)	1.1(1)	1.4(1)	1.5(1)

Table 5. Calorimetric data obtained for the studied garnets

Sample	*M*, g/mol	$H^0(973\ K) - H^0(298.15\ K) + \Delta_{dissol}H^0(973\ K)$	
		J/g	kJ/mol
I	501.25	897.3 ± 20.5 (9)*	449.8 ± 10.3
II	501.93	894.3 ± 15.6 (8)	448.9 ± 7.8
III	504.27	917.0 ± 15.7 (7)	462.4 ± 7.9
IV	510.43	911.3 ± 18.1 (9)	465.2 ± 9.2

* The errors are determined with 95% probability, numerals in parentheses are the numbers of the measurements.

the corresponding doublets (Table 3) were used to calculate the ratios $Fe^{(2+/3+)}/\sum Fe$ at sites *X, Y*, and *Z* with regard to corrections for the probabilities of the Mössbauer effect (*f*) at room temperature (Sawatzky et al., 1969; Schwartz et al., 1980)

$$f\left(Fe^{2+}(X)\right) = 0.78f\left(Fe^{3+}(Y)\right) = 0.78f\left(Fe^{2+}(Y)\right) = 0.73f\left(Fe^{3+}(Z)\right). \quad (2)$$

The calculated values of $Fe^{(2+/3+)}(X/Y/Z)/\sum Fe$ are reported in Table 4. In calculating the crystal chemical formulas, the obtained values of these ratios of doublets nos. 4 and 5 were equally divided between the corresponding crystallographic sites, analogously to what was done in (Schwartz et al., 1980).

The formulas of the studied samples of the titanium-bearing garnets calculated according to (Locock, 2008; Grew et al., 2013) and with regard to the results of all of the studies have the form

$(Ca_{3.00}Na_{0.02}Fe^{2+}_{0.01})(Fe^{3+}_{1.42}Ti^{4+}_{0.26}Al_{0.21}Mg_{0.04}Fe^{2+}_{0.03}Mn^{2+}_{0.01})[(Si_{2.85}Fe^{3+}_{0.13}O_{11.92}(OH)_{0.08}]$ (sample I),

$Ca_{3.01}\left(Fe^{3+}_{1.27}Ti^{4+}_{0.57}Mg_{0.05}Fe^{2+}_{0.03}Mn^{2+}_{0.01}\right)[(Si_{2.69}Al_{0.16}Fe^{3+}_{0.13}Ti^{4+}_{0.01})O_{11.96}(OH)_{0.04}]$ (sample II),

$(Ca_{2.97}Mn^{2+}_{0.02}Fe^{2+}_{0.01})(Fe^{3+}_{1.20}Ti^{4+}_{0.64}Mg_{0.05}Fe^{2+}_{0.04})[(Si_{2.64}Fe^{3+}_{0.23}Al_{0.11}Ti^{4+}_{0.01})O_{11.96}(OH)_{0.04}]$ (sample III),

$(Ca_{2.90}Na_{0.04}Fe^{2+}_{0.03}Mn^{2+}_{0.02}Mg_{0.01})(Fe^{3+}_{0.97}Ti^{4+}_{0.71}Mg_{0.13}Zr_{0.08}Fe^{2+}_{0.05})[(Si_{2.33}Fe^{3+}_{0.32}Ti^{4+}_{0.24}Al_{0.07})O_{11.84}(OH)_{0.16}]$ (sample IV).

The occupation of the crystallographic sites was carried out with regard to the Mössbauer spectroscopic data on the concentrations of the Fe^{2+} and Fe^{3+} cations at sites *X, Y*, and *Z*. If a sample was deficient in Si, the tetrahedral site of the sample was filled, in compliance with recommendations in (Huggins et al., 1977a), in the succession $Al^{3+} > Fe^{3+} > Ti^{4+}$. Titanium was introduced in such a way into site *Z* of samples II, III, and IV, which does not contradict either results in (Huggins et al., 1977a, 1977b; Tarte et al., 1979; Schwartz et al., 1980) or data of recent XAFS spectroscopic studies (Ackerson et al., 2017).

Thermochemistrty

Standard enthalpies of formation of the Ti-bearing garnets. The values of $\Delta_f H^0_{el}$ (298.15 K) were calculated from data of the thermochemical study of the minerals (Table 5) by reactions (3), (4), (5), and (6) and Eqs. (7) and (8).

For sample I

$$3CaO + 0.01Na_2O + 0.795Fe_2O_3 + 0.26TiO_2 + 0.092Al_2O_3 + 0.04MgO + 0.01MnO + 2.85SiO_2 + 0.027Al(OH)_3 = \left(Ca_{3.00}Na_{0.02}Fe^{2+}_{0.01}\right)\left(Fe^{3+}_{1.42}Ti^{4+}_{0.26}Al_{0.21}Mg_{0.04}Fe^{2+}_{0.03}Mn^{2+}_{0.01}\right)\left[\left(Si_{2.85}Fe^{3+}_{0.13}\right)O_{11.92}(OH)_{0.08}\right] + 0.01O_2, \quad (3)$$

Table 6. Thermochemical data used in calculating the enthalpy of formation (kJ/mol) of the studied garnets

Component	$H^0(973\ K) - H^0(298.15\ K) + \Delta_{dissol}H^0(973\ K)$	$-\Delta_fH^0(298.15\ K)$[a]
Na_2O(c)	-111.8 ± 0.8[b]	414.8 ± 0.3
MnO(c)	43.1 ± 0.8[c]	385.2 ± 0.5
CaO(c)	-21.78 ± 0.29[d]	635.1 ± 0.9
MgO(periclase)	36.38 ± 0.59[e]	601.6 ± 0.3
Fe_2O_3(hematite)	171.6 ± 1.9[f]	826.2 ± 1.3
Al_2O_3(corundum)	107.38 ± 0.59[g]	1675.7 ± 1.3
SiO_2(quartz)	39.43 ± 0.2[h]	910.7 ± 1.0
ZrO_2(baddeleyite)	62.44 ± 0.52[i]	1100.6 ± 1.7
TiO_2(rutile)	54.36 ± 1.47[j]	944.0 ± 0.8
$Al(OH)_3$(gibbsite)	172.6 ± 1.9[k]	1293.1 ± 1.2

[a]Tabulated data (Robie and Hemingway, 1995). [b]According to (Kiseleva et al., 2001). [c–j]Calculated using reference data on $[H^0(973\ K) - H^0(298.15\ K)]$ (Robie and Hemingway, 1995) and experimental dissolution data $\Delta_{dissol}H^0(973\ K)$: [c](Fritsch and Navrotsky, 1996); [d](Kiseleva et al., 1979); [e](Navrotsky and Coons, 1976); [f](Kiseleva, 1976); [g](Ogorodova et al., 2003); [h](Kiseleva et al., 1979); [i](Ellison and Navrotsky, 1992); [j](Xirouchakis et al., 1997). [k]According to (Ogorodova, 2011).

for sample II

$$3.01CaO + 0.715Fe_2O_3 + 0.58TiO_2 + 0.05MgO + 0.01MnO + 0.073Al_2O_3 + 2.69SiO_2 + 0.013Al(OH)_3 = Ca_{3.01}\left(Fe^{3+}_{1.27}Ti^{4+}_{0.57}Mg_{0.05}Fe^{2+}_{0.03}Mn^{2+}_{0.01}\right)\left[\left(Si_{2.69}Al_{0.16}Fe^{3+}_{0.13}Ti^{4+}_{0.01}\right)O_{11.96}(OH)_{0.04}\right] + 0.008O_2, \quad (4)$$

for sample III

$$2.97CaO + 0.02MnO + 0.74Fe_2O_3 + 0.65TiO_2 + 0.05MgO + 2.64SiO_2 + 0.048Al_2O_3 + 0.013Al(OH)_3 = \left(Ca_{2.97}Mn^{2+}_{0.02}Fe^{2+}_{0.01}\right)\left(Fe^{3+}_{1.20}Ti^{4+}_{0.64}Mg_{0.05}Fe^{2+}_{0.04}\right)\left[\left(Si_{2.64}Fe^{3+}_{0.23}Al_{0.11}Ti^{4+}_{0.01}\right)O_{11.96}(OH)_{0.04}\right] + 0.012O_2, \quad (5)$$

and for sample IV

$$2.90CaO + 0.02Na_2O + 0.02MnO + 0.14MgO + 0.685Fe_2O_3 + 0.95TiO_2 + 0.08ZrO_2 + 0.008Al_2O_3 + 2.33SiO_2 + 0.053Al(OH)_3 = \left(Ca_{2.90}Na_{0.04}Fe^{2+}_{0.03}Mn^{2+}_{0.02}Mg_{0.01}\right)\left(Fe^{3+}_{0.97}Ti_{0.71}Mg_{0.13}Zr_{0.08}Fe^{2+}_{0.05}\right)\left(Si_{2.33}Fe^{3+}_{0.32}Ti^{4+}_{0.24}Al_{0.07}\right)O_{11.84}(OH)_{0.16} + 0.02O_2, \quad (6)$$

$$\Delta_{r(1,2,3,4)}H^0(298.15\ K) = \left[\left(H^0(973\ K) - H^0(298.15\ K)\right)\right], \quad (7)$$

$$\Delta_f H^0_{el}(298.15\ K)_{garnet} = \Delta_{r(1,2,3,4)}H^0(298.15\ K) + \Sigma\nu_i\Delta_f H^0_{el}(298.15\ K)_{component\ i}, \quad (8)$$

where ν is the stoichiometric coefficients of reactions (3), (4), (5), and (6); $\Delta H = [(H^0(973\ K) - H^0(298.15\ K)) + \Delta_{dissol}H^0(973\ K)]$ is calorimetric data on the garnets (Table 5) and on the corresponding components of the reactions (Table 6); ΔH_{O_2} is the enthalpy $[(H^0(973\ K) - H^0(298.15\ K)]$ of O_2 compiled from (Robie and Hemingway, 1995); the required $\Delta_f H^0_{el}$ (298.15 K) values of the components of the reactions (oxides and Al hydroxide) are also reported in Table 6. Because oxidation of FeO makes it impossible to measure its dissolution heat in Pb borate melt, we assumed that Fe^{2+} contained in the garnet samples in small amounts (0.03–0.08 p.f.u.) can be regarded as Fe^{3+}. The obtained values of enthalpy of formation of the studied elements of titanium-bearing garnets are listed in Table 7.

Standard Gibbs energies of formation of the natural Ti-bearing garnets. To calculate the standard Gibbs energies of formation of the garnets from elements, we evaluated the standard entropy values not available from the literature (Table 7). In the calculations, we used the value $S^0(298.15\ K) = 324 \pm 2$ J/(K mol) for andradite, which was derived from measurements of the low-temperature heat capacity (Geiger et al., 2018). The calculations were carried out following the additive scheme and a model for evaluation of entropies of silicates proposed in (Holland, 1989), with the use of the values of the entropy contributions of oxides (*S-V*), with regard to the coordination of the corresponding cations in the structure of the mineral, where *S* and *V* are the entropy and volume of the oxides. We used (*S-V*)[gt] values for Mg, Ca, and Fe oxides proposed in (Holland, 1989) for garnets. For example, for sample I,

Table 7. Thermodynamic properties of Ti-bearing garnets at $T = 298.15$ K [a]

Mineral	$-\Delta_f H^{0}_{el}$ [b], kJ/mol	S^{0} [c], J/kmol	$-\Delta_f G^{0}_{el}$ [d], kJ/mol
Studied garnets			
$(Ca_{3.00}Na_{0.02}Fe^{2+}_{0.01})(Fe^{3+}_{1.42}Ti^{4+}_{0.26}Al_{0.21}Mg_{0.04}Fe^{2+}_{0.03}Mn^{2+}_{0.01}[(Si_{2.85}Fe^{3+}_{0.13})O_{11.92}(OH)_{0.08}]$ (I)	5861.1 ± 11.3	325.0 ± 2.2	5517.2 ± 11.3
$Ca_{3.01}\left(Fe^{3+}_{1.27}Ti^{4+}_{0.57}Mg_{0.05}Fe^{2+}_{0.03}Mn^{2+}_{0.01}\right)\left[\left(Si_{2.69}Al_{0.16}Fe^{3+}_{0.13}Ti^{4+}_{0.01}\right)O_{11.96}(OH)_{0.04}\right]$ (II)	5915.2 ± 9.0	328.0 ± 2.3	5572.6 ± 9.0
$\left(Ca_{2.97}Mn^{2+}_{0.02}Fe^{2+}_{0.01}\right)\left(Fe^{3+}_{1.20}Ti^{4+}_{0.64}Mg_{0.05}Fe^{2+}_{0.04}\right)\left[\left(Si_{2.64}Fe^{3+}_{0.23}Al_{0.11}Ti^{4+}_{0.01}\right)O_{11.96}(OH)_{0.04}\right]$ (III)	5902.5 ± 9.1	329.8 ± 2.3	5560.6 ± 9.1
$\left(Ca_{2.90}Na_{0.04}Fe^{2+}_{0.03}Mn^{2+}_{0.02}Mg_{0.01}\right)\left(Fe^{3+}_{0.97}Ti_{0.71}Mg_{0.13}Zr_{0.08}Fe^{2+}_{0.05}\right)\left[\left(Si_{2.33}Fe^{3+}_{0.32}Ti^{4+}_{0.24}Al_{0.07}\right)O_{11.84}(OH)_{0.16}\right]$ (IV)	5945.7 ± 10.2	345.8 ± 2.7	5605.1 ± 10.2
End members of the solid solutions			
$Ca_3Ti^{4+}_2[Fe^{3+}_2SiO_{12}]$ schorlomite	5775.0 ± 11.0	354.4 ± 3.8	5435.2 ± 11.0
$Ca_3(Ti^{4+}Fe^{2+})[Si_3O_{12}]$ morimotoite	6262.8 ± 10.2	342.9 ± 3.1	5925.6 ± 10.2

[a] Errors were calculated by the error propagation method. [b] Obtained in this study by the melt solution technique. [c] Evaluated using data on S^0(298.15 K) of andradite (Geiger et al., 2018). [d] Calculated by the equations $\Delta_f G = \Delta_f H - T\Delta_f S$.

$$\begin{gathered}Ca_3Fe_2^{3+}[Si_3O_{12}] + 0.01Na_2O + 0.04FeO + 0.26TiO_2 + 0.105Al_2O_3 + 0.04MgO \\ + 0.01MnO + 0.04H_2O \\ = (Ca_{3.00}Na_{0.02}Fe^{2+}_{0.01})(Fe^{3+}_{1.42}Ti^{4+}_{0.26}Al_{0.21}Mg_{0.04}Fe^{2+}_{0.03}Mn^{2+}_{0.01})[(Si_{2.85}Fe^{3+}_{0.13})O_{11.92}(OH)_{0.08}] \\ + 0.225Fe_2O_3 + 0.15SiO_2,\end{gathered} \quad (9)$$

$$\begin{gathered}S^0(298.15\ K)_{garnet} = S^0(298.15\ K)_{andradite} \\ + 0.01(S\text{-}V)^{[8]}Na_2O + 0.04(S\text{-}V)^{[grt]}FeO \\ + 0.26(S\text{-}V)^{[6]}TiO_2 + 0.105(S\text{-}V)^{[6]}Al_2O_3 \\ + 0.04(S\text{-}V)^{[grt]}MgO + 0.01(S\text{-}V)^{[6]}MnO \\ + 0.04SH_2O - 0.225(S\text{-}V)^{[6]}Fe_2O_3 \\ - 0.15(S\text{-}V)^{[4]}SiO_2,\end{gathered} \quad (10)$$

where the coordination numbers of cations in the garnet structure are specified in brackets, and the values of (S-V) were borrowed from (Holland, 1989).

The values of the Gibbs standard energy of formation of the natural garnets from elements (Table 7) were calculated using the obtained values of S^0 (298.15 K) and $\Delta_f H^0_{el}$ (298.15 K).

Thermodynamic properties of the end members of the solid solution series. Using our calorimetric data on the titanium-bearing garnets, we have calculated the enthalpies of formation of the end members of the isomorphous series andradite–schorlomite–morimotoite. To do this, we recalculated the experimental data on sample IV into the molecular weights of schorlomite (M = 547.77 g/mol) and morimotoite (M = 500.21 g/mol). The enthalpies of their formation were calculated using equations analogous to Eqs. (3)–(8). The standard entropies of these minerals (absent from the literature) were evaluated analogously to what had been done for natural garnets, using data on S^0(298.15 K) of andradite (Geiger et al., 2018). The results are summarized in Table 7. The calculated values of S^0(298.15 K) and $\Delta_f H^0_{el}$ (298.15 K) enabled us to calculate the Gibbs free energies of formation of schorlomite and morimotoite from elements (Table 7).

THERMODYNAMIC SIMULATION OF THE STABILITY FIELDS OF TITANIUM-BEARING GARNETS

Titanium-bearing garnets were found at numerous localities worldwide. In Russia, they are known to occur in massifs of the Maimecha–Kotui alkaline province in Krasnoyarsk Kray, northern central Siberia (Odikhincha, Guli, and Kugda); in the Karelian–Kola alkaline province (Afrikanda, Kovdor, massifs in the Turii Peninsula, Vuorijärvi, Khibina, etc.); massifs in the Sangilen Highland, Tyva, southern central Siberia (Dakhu-Nuur, Chik Khen, etc.); in the Aldan Shield in Yakutia; and in the Zhidoi massif in Irkutsk oblast in central southern Siberia. These minerals were found abroad in the United States (in the Magnet Cove and Hot Spring alkaline massifs in Arkansas and in the Gem Mine and San Benito massifs in California), Sweden (Alnö Island), Scotland (Camphouse, Ardnamurchan, and Argyllshire), Finland (Iivaara and Kuusamo), Japan (Fuka and Bicchu in Okayama Prefecture), Brazil (Jacupiranga Mine, São Paulo), China (Fanshan ultramafic complex in Hebei Province), New Zealand (Tokatoka district, Auckland) and many others. Garnets enriched in Ti occur in associations with nepheline, diopside, apatite, calcite, minerals of the melilite group, phlogopite, perovskite, etc. Garnets of the andradite–schorlomite–morimotoite series are formed in melilite rocks only in their contact zones with ijolites–melteigites.

Thermodynamic data obtained for Ti-rich garnets were used to model phase relations in the system TiO_2–SiO_2–Al_2O_3–Fe_2O_3–FeO–CaO–MgO–Na_2O–CO_2. The principal reactions forming Ti-bearing garnets in melilite–perovskite rocks are as follows:for the end members of the schorlomite–morimotoite series

$$\begin{gathered}\underset{\text{perovskite }(Prv)}{2CaTiO_3} + \underset{\text{melilite }(Mll)}{2Ca_{1.5}Na_{0.5}Al_{0.5}Mg_{0.5}Si_2O_7} + \underset{\text{hematite }(Hem)}{Fe_2O_3} + CO_2 \\ \underset{\text{schorlomite }(Shr)}{Ca_3Ti_2[(SiFe_2^{3+})O_{12}]} + \underset{\text{nepheline }(Nph)}{NaAlSiO_4} + \underset{\text{calcite }(Cal)}{CaCO_3} + \underset{\text{diopside }(Di)}{CaMgSi_2O_6},\end{gathered} \quad (11)$$

$$\begin{gathered}\underset{\text{perovskite }(Prv)}{CaTiO_3} + 4\underset{\text{melilite }(Mll)}{Ca_{1.5}Na_{0.5}Al_{0.5}Mg_{0.5}Si_2O_7} + \underset{\text{magnetite }(Mag)}{FeFe_2O_4} \\ + 2CO_2 = \underset{\text{morimotoite }(Mrm)}{Ca_3TiFe^{2+}[Si_3O_{12}]} + 2\underset{\text{nepheline }(Nph)}{NaAlSiO_4} \\ + \underset{\text{diopside }(Di)}{CaMgSi_2O_6} + \underset{\text{monticellite }(Mll)}{CaMgSiO_4} + \underset{\text{hematite }(Hem)}{Fe_2O_3} + 2\underset{\text{calcite }(Cal)}{CaCO_3},\end{gathered} \quad (12)$$

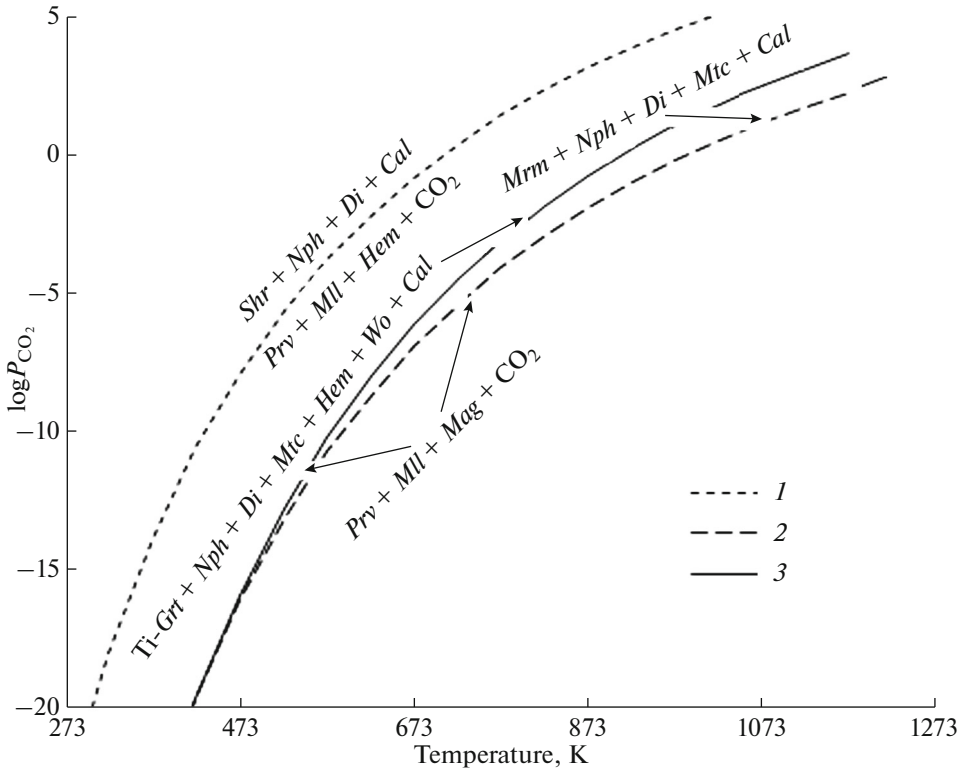

Fig. 6. Stability fields of Ti-bearing garnets. Line *1* corresponds to reaction (1), line *2* corresponds to reaction (12), and line *3* corresponds to reaction (13).

and for garnet of intermediate composition

$$\underset{\text{perovskite}(Prv)}{CaTiO_3} + 4\underset{\text{melilite}(Mll)}{Ca_{1.5}Na_{0.5}Al_{0.5}Mg_{0.5}Si_2O_7} + \underset{\text{magnetite}(Mag)}{0.5FeFe_2O_4} + 1.5CO_2$$
$$= \underset{\text{Ti-garnet (Ti-}Grt)}{Ca_3TiFe^{2+}_{0.5}Fe^{3+}_{0.5}\left[\left(Si_{2.5}Fe^{3+}_{0.5}\right)O_{12}\right]} + \underset{\text{nepheline }(Nph)}{2NaAlSiO_4} + \underset{\text{diopside }(Di)}{CaMgSi_2O_6} \quad (13)$$
$$+ \underset{\text{monticellite }(Mtc)}{CaMgSiO_4} + \underset{\text{wollastonite }(Wo)}{0.5CaSiO_3} + \underset{\text{hematite }(Hem)}{Fe_2O_3} + \underset{\text{calcite }(Cal)}{1.5CaCO_3}.$$

Melilite of hypothetical composition involved in reactions (11)–(13) is close in composition to the naturally occurring melilite, which is most often found in association with Ti-bearing garnets, and the composition of the Ti-bearing garnet is close to the real composition of sample IV. The *P*–*T* parameters of mineral equilibria according to reactions (11)–(13) were calculated by the HCh (Shvarov, 2008) program package, with thermodynamic constants of components of the reactions compiled from (Holland and Powell, 1998). The thermodynamic parameters of melilite were calculated from experimental thermochemical data on melilite of analogous composition in (Ogorodova et al., 2018), and data on Ti-bearing garnet were calculated according to an algorithm for calculating thermodynamic parameters of the end members of the schorlomite–morimotoite series.

The stability fields of the mineral assemblages obtained by the simulations (Fig. 6) show that garnet of chemical composition close to that of sample IV is stable at a lower temperature than morimotoite but at a much higher temperature than schorlomite of idealized composition. It should be mentioned that no garnets of the schorlomite–morimotoite isomorphous series have been found in nature as of yet. However, analogues of schorlomite and almost all intermediate members of the schorlomite–andradite series have been synthesized (Ito and Frondel, 1967). Moreover, garnets of intermediate composition of the grandite (andradite + grossular)–schorlomite–morimotoite series have also been synthesized (Henmi et al., 1995). All attempts to synthesize morimotoite have so far failed.

This publication presents thermodynamic characteristics of titanium-bearing garnets that have been obtained for the first time in experiments with naturally occurring samples. Using our data, we have also calculated the thermodynamic characteristics of the end members of the isomorphic series schorlomite–

morimotoite. These values can be recommended to be used in developing thermodynamic models for the origin of minerals and mineral assemblages with Ti-bearing garnets in nature.

ACKNOWLEDGMENTS

The authors thank the staff of Fersman Mineralogical Museum, Russian Academy of Sciences, for providing samples for this research. D.A. Khanin is thanked for conducting chemical analyses of the minerals.

FUNDING

This study was supported by Russian Foundation for Basic Research, project no. 18-29-12128 mk.

CONFLICT OF INTEREST

The authors declare that they have no conflicts of interest.

REFERENCES

M. R. Ackerson, N. D. Tailby, and E. B. Watson, "XAFS spectroscopic study of Ti coordination in garnet," Am. Mineral. **102**, 173–183 (2017).

S. M. Antao, S. Mohib, M. Zaman, and R. A. Marr, "Ti-rich andradites: chemistry, structure, multi–phases, optical anisotropy, and oscillatory zoning," Can. Mineral. **53**, 133–158 (2015).

T. Armbruster, J. Birrer, E. Libowitzky, and A. Beran, "Crystal chemistry of Ti–bearing andradites," Eur. J. Mineral. (10), 907–921 (1998).

A. R. Chakhmouradian and C. A. McCammon, "Schorlomite: a discussion of the crystal chemistry, formula, and inter-species boundaries," Phys. Chem. Miner. **32**, 277–289 (2005).

N. V. Chukanov, *Infrared Spectra of Mineral Species: Extended Library* (Springer-Verlag GmbH, Dordrecht–Heidelberg–N.Y.–London, 2014)

B. Z. Dilnesa, B. Lothenbach, G. Renaudin, G. Wichser, and D. Kulik, "Synthesis and characterization of hydrogarnet $Ca_3(Al_xFe_{1-x})_2(SiO_4)_y(OH)_{4(3-y)}$," Cem. Concr. Res. **59**, 96–111 (2014).

E. Dowty, "Crystal chemistry of titanian and zirconian garnet: I. Review and spectral studies," Am. Mineral. **56**, 1983—2009 (1971).

A. J. G. Ellison and A. Navrotsky, "Enthalpy of formation of zircon," J. Am. Ceram. Soc. **75**, 1430–1433 (1992).

S. Fritsch and A. Navrotsky, "Thermodynamic properties of manganese oxides," J. Am. Ceram. Soc. **79**(7), 1761–1768 (1996).

I. Galuskina, E. Galuskin, Y. Vapnik, G. Zeliński, and K. Prusik, "Priscillagrewite-(Y), IMA 2020-002," CNMNC Newslett. No. 55. Mineral. Mag. **84** (3), (2020).

C. A. Geiger, E. Dachs, N. M. Vielreicher, and G. R. Rossman, "Heat capacity and entropy behavior of andradite: a multy-sample and methodological investigation," Eur. J. Mineral. **30**, 681–694 (2018).

E. S. Grew, A. J. Locock, S. J. Mills, I. O. Galuskina, E. V. Galuskin, and U. Halenius, "Nomenclature of the garnet supergroup," Am. Mineral. **98**, 785–811 (2013).

Yu. D. Gritsenko, "Titanium garnets collection of the A. E. Fersman Mineralogical Museum of the Russian Academy of Sciences," New Data on Minerals **52** (1), 3–5 (2018).

C. Henmi, I. Kusachi, and K. Henmi, "Morimotoite, $Ca_3TiFe^{2+}Si_3O_{12}$, a new titanian garnet from Fuka, Okayama Prefecture, Japan," Mineral. Mag. **59**, 115–120 (1995).

A. M. Hofmeister and A. Chopelas, "Vibrational spectroscopy of end-member silicate garnets," Phys. Chem. Mineral. **17**, 503–526 (1991).

T. J. B. Holland, "Dependence of entropy on volume for silicate and oxide minerals: A review and a predictive model," Am. Mineral. **74**, 5–13 (1989).

T. J. B. Holland and R. Powell, "An internally consistent thermodynamic data set for phases of petrological interest," Metamorph. Geol. **16**, 309–343 (1998).

F. E. Huggins, D. Virgo, and H. G. Huckenholz, "Titanium-containing silicate garnets. I. The distribution of Al, Fe^{3+}, and Ti^{4+} between octahedral and tetrahedral sites," Am. Mineral. **62**, 475–490 (1977a).

F. E. Huggins, D. Virgo, and H. G. Huckenholz, "Titanium-containing silicate garnets. II. The crystal chemistry of melanites and schorlomites," Am. Mineral. **62**, 646–665 (1977b).

IMA List of Minerals. http://cnmnc.main.jp/IMA_Master_List_(2020-1).pdf

J. Ito and C. Frondel, "Synthetic zirconium and titanium garnets," Am. Mineral. **52**, 773–781 (1967).

A. Karlsson, D. Holtstam, L. Bindi, P. Bonazzi, and M. Konrad-Schmolke, "Adding complexity to the garnet supergroup: monteneveite, $Ca_3Sb_2^{5+}\left(Fe_2^{3+}Fe^{2+}\right)O_{12}$, a new mineral from the Monteneve mine, Bolzano Province, Italy," Eur. J. Mineral. **32**, 77–87 (2020).

A. Katerinopoulou, A. Katerinopoulos, P. Voudouris, A. Bieniok, M. Musso, and G. Amthauer, "A multi–analytical study of the crystal structure of unusual Ti–Zr–Cr–rich andradite from the Maronia skarn, Rhodope massif, western Thrace, Greece," Mineral. Petrol. **95**, 113–124 (2009).

I. A. Kiseleva, "Thermodynamic properties and pyrope stability," Geokhimiya, No. **6**, 845–854 (1976).

I. A. Kiseleva and L. P. Ogorodova, "Application of high-temperature solution calorimetry for the determination of enthalpies of formation of hydroxyl-bearing minerals: evidence from talck and tremolite," Geokhimiya, (12), 1745–1755 (1983).

I. A. Kiseleva, L. P. Ogorodova, N. D. Topor, and O. G. Chigareva, "Thermochemical study of the CaO–MgO–SiO_2 system," Geokhimiya, No. **12**, 1811–1825 (1979).

I. A. Kiseleva, A. Navrotsky, I. A. Belitsky, and B. A. Fursenko, "Thermochemical study of calcium zeolites – heulandite and stilbite," Am. Mineral. **86**, 448–455 (2001).

B. A. Kolesov and C. A. Geiger, "Raman spectra of silicate garnets," Phys. Chem. Mineral. **25**, 142–151 (1998).

S. V. Krivovichev, V. N. Yakovenchuk, T. L. Panikorovsky, E. E. Savchenko, Ya. A. Pakhomovsky, Yu. A. Mikhai-

lova, E. A. Selivanova, G. I. Kadyrova, and G. Yu. Ivanyuk, "Nickelmelnikovite $Ca_{12}Fe^{2+}Fe^{3+}_3Al_3(SiO_4)_6(OH)_{20}$: a new mineral from the Kovdor massif (Kola Peninsula, Russia)," Dokl. Earth Sci. **488** (2), 1200–1202 (2019).

V. S. Kurashkovskaya and E. Yu. Borovikova, "IR spectra of grossular–andradite granets," Zap. Ross. Mineral. O-va, No. 5, 70–75 (2002).

A. J. Locock, "An Excel spreadsheet to recast analyses of garnet into end-member components, and a synopsis of the crystal chemistry of natural silicate garnets," Comput. Geosci. **34**, 1769–1780 (2008).

A. Locock, R. W. Luth, R. G. Cavell, D. G. W. Smith, and M. J. M. Duke, "Spectroscopy of the cation distribution in the schorlomite species of garnet," Am. Mineral. **80**, 27–38 (1995).

C. Ma and A. N. Krot, "Hutcheonite, $Ca_3Ti_2(SiAl_2)O_{12}$, a new garnet mineral from the Allende meteorite: An alteration phase in a Ca-Al-rich inclusion," Am. Mineral. **99**, 667–670 (2014).

M. E. Matsnev and V. S. Rusakov, "SpectrRelax – an application for Mössbauer spectra modeling and fitting," AIP Conf. Proc. **1489**, 178–185 (2012). https://doi.org/10.1063/1.4759488

F. Menil, "Systematic trends of the ^{57}Fe Mössbauer isomer shifts in (FeO_n) and (FeF_n) polyhedra. Evidence of a new correlation between the isomer shift and the inductive effect of the competing bond T–X (→Fe) (where X is O or F and T any element with a formal positive charge)," J. Phys. Chem. Solids. **46**, 763–789 (1985).

MINCRYST Crystallographic and Crystallochemical Database for Minerals and their Structural Analogues. http://database.iem.ac.ru/mincryst/rus/search.php

R. K. Moore and W. B. White, "Vibrational spectra of the common silicates: I. The garnets," Am. Mineral. **56**, 54–71 (1971).

A. Navrotsky and W. E. Coons, "Thermochemistry of some pyroxenes and related compounds," Geochim. Cosmochim. Acta. **40**, 1281–1290 (1976).

L. P. Ogorodova, I. A. Kiseleva, L. V. Mel'chakova, M. F. Vigasina, and E. M. Spiridonov, "Calorimetric determination of the enthalpy of formation for pyrophyllite," Russ. J. Phys. Chem. A **85** (9), 1492–1494 (2011).

L. P. Ogorodova, L. V. Melchakova, I. A. Kiseleva, and I. A. Belitsky, "Thermochemical study of natural pollucite," Thermochim. Acta. **403**, 251–256 (2003).

L. P. Ogorodova, Yu. D. Gritsenko, M. F. Vigasina, A. Yu. Bychkov, D. A. Ksenofontov, and L. V. Melchakova, "Thermodynamic properties of natural melilites," Am. Mineral. **103**, 1945–1952 (2018).

R. C. Peterson, A. J. Locock, and R. W. Luth, "Positional disorder of oxygen in garnets: the crystal–structure refinement of schorlomite," Can. Mineral. **33**, 627–631 (1995).

K. F. Rammelsberg, "Analysis of the schorlomite of Shepard," Am. J. Sci. Arts. **9**, 429 (1850).

I. T. Rass and L. S. Dubrovinskii, "The thermodynamic parameters and stability region of schorlomite," Dokl. Earth Sci. **354** (6), 730–732 (1997).

J. M. Rivas-Mercury, P. Pena, A. de Aza, and X. Turrillas, "Dehydration of $Ca_3Al_2(SiO_4)_y(OH)_{4(3-y)}$ ($0 < y < 0.176$) studied by neutron thermodiffractometry," J. Eur. Ceram. Soc. **28**, 1737–1748 (2008).

R. A. Robie and B. S. Hemingway, "Thermodynamic properties of minerals and related substances at 298.15 K and 1 bar (10^5 pascals) pressure and at higher temperatures," US Geol. Surv. Bull. **2131,** (1995). RRUFF Database of Raman Spectroscopy, X–ray Diffraction and Chemistry of Minerals. http://www.rruff.info.

G. A. Sawatzky, F. van der Woude, and A. H. Morrish, "Recoilless–fraction ratios for ^{57}Fe in octahedral and tetrahedral sites of a spinel and a garnet," Phys. Rev. **183**, 383–386 (1969).

E. Schingaro, F. Scordary, G. Pedrazzi, and C. Malitesta, "Ti and Fe Speciation by X-ray photoelectron spectroscopy (XPS) and Mössbauer spectroscopy for a full crystal chemical characterization of Ti-garnets from Colli Albani (Italy)," Ann. Chim. **94**, 185–196 (2004).

E. Schingaro, M. Lacalamita, E. Mesto, G. Ventruti, G. Pedrazzi, L. Ottolini, and F. Scordary, "Crystal chemistry and light elements analysis of Ti-rich garnets," Am. Mineral. **101**, 371–384 (2016).

K. B. Schwartz, D. A. Nolet, and R. G. Burns, "Mössbauer spectroscopy and crystal chemistry of natural Fe–Ti garnets," Am. Mineral. **65**, 142–153 (1980).

C. U. Shepard, "On three new mineral species from Arkansas, and the discovery of the diamond in North Carolina," Am. J. Sci. **2**, 249–250 (1846).

Yu. V. Shvarov, "HCh: New potentialities for the thermodynamic simulation of geochemical systems offered by Windows," Geochem. Int. **46** (8), 834–839 (2008).

P. Tarte, R. Cahay, and A. Garcia, "Infrared spectrum and structural role of titanium in synthetic Ti-garnets," Phys. Chem. Miner. **4**, 55–63 (1979).

J. D. Whitney, "Examination of three new mineralogical species proposed by Professor C. U. Shepard," J. Natural Boston **6**, 42–48 (1849).

D. Xirouchakis, S. Fritsch, R. L. Putnam, A. Navrotsky, and D. H. Lindsley, "Thermochemistry and the enthalpy of formation of synthetic end–member ($CaTiSiO_5$) titanite," Am. Mineral. **82**, 754–759 (1997).

H. Xu, P. J. Heaney, A. Navrotsky, L. Topor, and J. Liu, "Thermochemistry of stuffed quartz-derivative phases along the join $LiAlSiO_4$–SiO_2," Am. Mineral. **84**, 1360–1369 (1999).

Translated by E. Kurdyukov